Int. J. Heat Mass Transfer. Vol. 34, No. 2, pp. 513–524, 1991
Printed in Great Britain

0017–9310/91 $3.00+0.00

Laminar thermal convection between vertical coaxial isothermal cylinders

RANGANATHAN KUMAR and M. A. KALAM
Department of Mechanical Engineering, Clemson University, Clemson, SC 29631, U.S.A.

(*Received* 16 *September* 1988 *and in final form* 17 *April* 1990)

Abstract—A numerical investigation of natural convective heat transfer of a fluid in vertical cylindrical annuli with the inner wall maintained at a higher temperature than the outer wall has been carried out. The top and the bottom plates are insulated for the majority of the cases. Perfectly conducting horizontal walls are also considered for comparison of heat transfer results. Numerical results of heat transfer rates and flow fields for $10 \leqslant Ra_L \leqslant 10^6$, $1 \leqslant \kappa \leqslant 15$ and $0.3 \leqslant A \leqslant 10$ are reported. Discrepancies in the existing numerical and experimental data are noted and discussed. New correlations for heat transfer rate are given.

INTRODUCTION

NATURAL convection in vertical annular spaces has been studied both experimentally and numerically by a number of researchers. The first extensive study of natural convection in isothermally heated vertical annuli was reported by de Vahl Davis and Thomas [1] and the parametric studies were further extended by the same authors [2]. Although a wide range of parameters was used, not all combinations were investigated. Based on their numerical data for $Ra_L \leqslant 2\times10^5$, $0.5 < Pr < 10^4$, $1 \leqslant A \leqslant 33$, they obtained a heat transfer correlation in the boundary layer regime

$$Nu_L = 0.286 Ra_L^{0.258}\, Pr^{0.006}\, A^{-0.238} \kappa^{0.442}. \quad (1)$$

The first experiment to show the diameter ratio effect was performed by Prasad and Kulacki [3]. Their experiments were conducted for $8\times10^6 < Ra_L < 3\times10^{10}$, $\kappa = 5.338$, aspect ratios of 0.5, 1 and 1.5, and Prandtl number range of $4 < Pr < 196$. Curvature effects on the temperature field were found to be significant and the difference between their results and the correlation equation (1) obtained by ref. [2] was as high as 60%. The discrepancies in the results reported by the two papers will be discussed in this paper. The heat transfer correlation equation (1) was tested with the experimental data of Emery and Chu [4] and the numerical data of Rubel and Landis [5] for $\kappa = 1$ and the results were found to be in good agreement. However, $\kappa = 1$ takes the diameter ratio effect out of the correlation and the agreement in results are valid only for plane vertical layers.

In the results reported by de Vahl Davis and Thomas [1] for $A \geqslant 5$ and $\kappa = 2$ at moderate Rayleigh numbers, the motion consists of a single cell, i.e. a torus, while at high Rayleigh numbers, multicellular motion is observed. A similar phenomenon was reported by Elder [6]. He observed experimentally a weak multicellular motion superimposed on a steady unicellular pattern at high aspect ratios (up to 60) and high Prandtl number (up to 1000). Lee *et al.* [7] numerically studied the structure of multicellular convection in tall vertical annuli for $10 \leqslant A \leqslant 20$, $0 \leqslant Pr \leqslant 0.7$, and $1 \leqslant \kappa \leqslant 5$. A Prandtl number of zero represents a hypothetical fluid with infinite thermal diffusivity. They reported multicelluar flow in air that drifted upwards whenever $A > 13$. Choi and Korpela [8] studied the instability in the conduction flow regime in tall vertical annuli using the linear perturbation theory. They reported that for low Prandtl number fluids, the curvature has a stabilizing effect on the flow; however, the effect is reversed for high Prandtl number flows.

Nagendra *et al.* [9] developed an approximate analysis for the isothermally heated annuli by extending the approximate boundary layer model used by Emery and Chu [4]. They presented three heat transfer correlations in the laminar boundary layer regime of convection for small and large aspect ratios. A large discrepancy in the energy balance is a shortcoming of their analysis. Schwab and DeWitt [10] provided heat transfer results that were limited to 24 combinations of Ra_L, Pr and A with $\kappa = 2$.

A few papers appear in the literature which deal with isoflux heating of the inner cylinder. Sheriff [11] conducted experiments for very high aspect ratios and diameter ratios close to unity. Keyhani *et al.* [12] made heat transfer measurements for a diameter ratio significantly higher than unity ($\kappa = 4.33$), $A = 27.6$ and $10^3 < Ra_L < 2.3\times10^6$. Bhushan *et al.* [13] extended the work of Keyhani *et al.* [12] for two other combinations of diameter and aspect ratio. A detailed parametric study of natural convection in a vertical annulus with isoflux heating on the inner wall and isothermal cooling on the outer was carried out by Khan and Kumar [14]. The results compared well with the experimental results of Keyhani *et al.* [12].

The available heat transfer correlation given in equation (1) overpredicts the heat transfer rate and hence a systematic parametric study needs to be per-

NOMENCLATURE

A	aspect ratio
C_p	specific heat
$\mathbf{F}$	body force
g	acceleration due to gravity
$\bar{h}$	average heat transfer coefficient on the inner wall
k	thermal conductivity of the fluid
L	gap width, $r_o - r_i$
Nu_L	Nusselt number, $\bar{h}L/k$
Nu_{d_i}	Nusselt number, $\bar{h}d_i/k$
P	pressure
Pr	Prandtl number, ν/α
q	constant heat flux applied on the inner wall
r	radial coordinate
R	dimensionless radial coordinate, r/L
Ra_L	Rayleigh number, $\beta g(\Delta T)L^3/\alpha\nu$
Ra_{d_i}	Rayleigh number, $\beta g(\Delta T)d_i^3/\alpha\nu$
T	dimensional temperature
ΔT	temperature difference across the annulus
V_R	non-dimensional radial velocity, $V'_R L/\alpha$
V_z	non-dimensional radial velocity, $V'_z L/\alpha$
V	velocity vector
V'_R	dimensional radial velocity
V'_z	dimensional vertical velocity
z	vertical coordinate.

Greek symbols

α	thermal diffusivity
β	coefficient of volumetric expansion
ζ	vorticity
κ	radius ratio, $r_o - r_i$
ξ	vector potential
ρ	density
τ	dimensionless temperature, $(T-T_o)/(T_i-T_o)$
ψ	stream function.

Subscripts

C	conduction
d_i	based on inner diameter
H	height of the cylinders
i	inner wall
L	based on gap width
o	outer wall.

formed. Also, the only data available for $A < 1$ are the experimental data given by Prasad and Kulacki [3] for $A = 0.5$ and $Ra_L > 10^7$. The objectives in this paper are to present numerical results from finite difference calculations of natural convection for isothermally heated vertical cylinders for $1 \leqslant \kappa \leqslant 15$, $0.3 \leqslant A \leqslant 10$ and $10 \leqslant Ra_L \leqslant 10^6$, and to provide heat transfer correlations for low and medium aspect ratios.

MATHEMATICAL FORMULATION

The governing equations for a steady, laminar flow with negligible viscous dissipation and no heat generation, may be written as follows:

continuity

$$\nabla \cdot \mathbf{V} = \mathbf{0} \tag{2}$$

momentum

$$\rho(\mathbf{V}\cdot\nabla)\mathbf{V} = -\nabla p + \mathbf{F} - \mu\nabla\times(\nabla\times\mathbf{V}) \tag{3}$$

energy

$$\rho c_p(\mathbf{V}\cdot\nabla)T = k(\nabla\cdot\nabla)T \tag{4}$$

where $\mathbf{F}$ is the body force given by

$$\mathbf{F} = \rho g.$$

Using the annular width, L, as the non-dimensional parameter, the annulus is found to be bound by $R = r_i/L$ on the inner cylinder and $R = r_o/L$ at the outer cylinder. In the vertical direction, Z varies from 0 to A $(= z_{max}/L)$. The inner wall is at a constant temperature, T_i, and the outer wall at a constant temperature, T_o.

The dimensionless quantities are

$$V_R = \frac{V'_R L}{\alpha}; \quad V_z = \frac{V'_z L}{\alpha}$$

$$R = \frac{r}{L}; \quad \tau = \frac{T-T_o}{T_i-T_o}$$

$$Ra_L = \frac{\beta g(\Delta T)L^3}{\alpha\nu}; \quad \kappa = \frac{r_o}{r_i}; \quad A = \frac{Z_{max}}{L}. \tag{5}$$

The Navier–Stokes equations are recast as vorticity–stream function equations. The following equations relate velocity $\mathbf{V}$ to vorticity ζ and vector potential ξ

$$\mathbf{V} = \nabla\times\xi$$

$$\zeta = \nabla\times\mathbf{V}. \tag{6}$$

The azimuthal component of ξ in two-dimensional flows is the stream function and henceforth will be denoted by ψ. ζ is the azimuthal component of vorticity.

Using the non-dimensional parameters, the final set of equations to be solved are (for a Boussinesq fluid)

$$\frac{\partial^2\psi}{\partial z^2} + \frac{\partial^2\psi}{\partial R^2} + \frac{1}{R}\frac{\partial\psi}{\partial R} - \frac{\psi}{R^2} = -\zeta \tag{7}$$

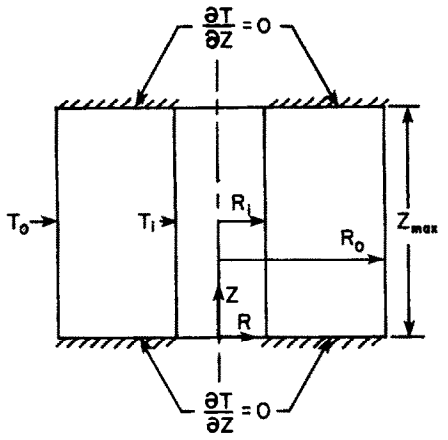

FIG. 1. The geometry and the coordinate system.

$$\frac{\partial}{\partial z}(V_z\zeta)+\frac{\partial}{\partial R}(V_R\zeta) = -Ra_L\, Pr\frac{\partial \tau}{\partial R} + Pr\left\{\frac{\partial^2\zeta}{\partial z^2}+\frac{\partial^2\zeta}{\partial R^2}+\frac{1}{R}\frac{\partial\zeta}{\partial R}-\frac{\zeta}{R^2}\right\} \quad (8)$$

$$\left(V_R\frac{\partial\tau}{\partial R}+V_z\frac{\partial\tau}{\partial z}\right)=\left(\frac{\partial^2\tau}{\partial R^2}+\frac{1}{R}\frac{\partial\tau}{\partial z}+\frac{\partial^2\tau}{\partial z^2}\right). \quad (9)$$

The boundary conditions for the problem (Fig. 1) can be written using no-slip conditions for velocity, constant temperature on the inner and outer cylinders, and insulated condition on the horizontal walls as shown in Table 1. Some results are also obtained for a perfectly conducting wall condition at $Z = 0$ and A where the temperature is allowed to vary linearly from 1 to 0 from the inner to the outer cylinder. The overall Nusselt numbers for each wall are given by

$$Nu_i = -\frac{1}{A}\int_0^A \left.\frac{\partial\tau}{\partial R}\right|_i dZ$$

$$Nu_o = -\frac{1}{A}\int_0^A \left.\frac{\partial\tau}{\partial R}\right|_o dZ. \quad (10)$$

NUMERICAL PROCEDURE AND VALIDATION

A numerical solution based on the false transient method and alternating direction implicit (ADI) scheme has been used to solve the vorticity transport and energy equations. Specifically, equations (8) and (9) were made parabolic by the inclusion of pseudo-time-dependent terms, $(Pr/\alpha_\zeta)/(\partial\zeta/\partial t)$ and $(1/\alpha_\zeta)/(\partial\tau/\partial t)$ to the left-hand sides of the vorticity and energy equations. The specific derivation of the ADI method was a variation of the one proposed by Samarskii and Andreyev [15]. The factors α_ζ and α_τ were adjusted to reach a steady state. Typically, the value of both α_ζ and α_τ was 0.05 and Δt was set equal to 0.004 for $Ra_L \leqslant 5\times10^4$. For $Ra_L \geqslant 5\times10^4$, α_ζ was usually reduced to 0.025 and Δt was kept at 0.0015 to speed up convergence. The stream function equation was solved by the successive over-relaxation (SOR) method.

Table 1. Boundary conditions

	$R = R_i$	$R = R_o$	$Z = 0$	$Z = A$
τ	$\tau = 1$	$\tau = 0$	$\partial\tau/\partial z = 0$	$\partial\tau/\partial z = 0$
ζ	$-\partial^2\psi/\partial R^2$	$-\partial^2\psi/\partial R^2$	$-\partial^2\psi/\partial z^2$	$-\partial^2\psi/\partial z^2$
ψ	0	0	0	0

The choice of the diameter ratio, κ, the aspect ratio, A, and the Rayleigh number, Ra_L, determined the type of mesh to be used. The uniform and semi-uniform meshes employed in the present study are: $R\times Z$: 21×21, 26×26, 27×41, 41×41 and 27×97. Uniform meshes have been used for Rayleigh numbers less than 2×10^4 in some cases and less than 5×10^4 in other cases and, semi-uniform meshes have been used for higher Rayleigh numbers. In the semi-uniform mesh system, the grid was closely spaced near the walls, with the ratio of adjacent grid spacing maintained below 1.5, and uniformly spaced in the core of the annulus. The following criterion was used for checking convergence at each point:

$$|\phi_{new}-\phi_{old}|/|\phi_{new}|_{max} \leqslant \Gamma \quad (11)$$

where ϕ was the primary variable being tested and Γ was a prespecified constant, usually set at 10^{-3}. The agreement between the energy input at the inner cylinder and the energy output at the outer cylinder was also used to check the validity of the numerical scheme. The convergence parameter, Γ, was frequently reduced from 10^{-3} to 10^{-4} to maintain the energy balance within 2%. For uniform mesh, the convergence test was applied to ζ, τ and ψ. For semi-uniform mesh, V_R, V_z and τ were tested. At high Ra_L, that is, when the semi-uniform mesh is used, the vorticity boundary values do not readily stabilize in the numerical solution. Since the velocities have more of a physical significance, and are more stable near the boundaries, the test for convergence is applied against the velocities in more severe flow situations.

The numerical code used has been validated by generating heat transfer results and comparing with published data. Heat transfer results obtained in the present study for a square cavity using the grids (21×21) and (41×41) compared very well with the solution [16] and the benchmark solution of de Vahl Davis [17]. These cavity results and some specific results generated for $\kappa = 2$ and $A = 10$ and compared with the results of de Vahl Davis and Thomas [1] are shown in Table 2. Several grids had been chosen for various diameter ratios and aspect ratios, and in all cases, grid independence of results was checked and ensured. An NAS AS/XL-V60 computer was used for all computations.

RESULTS AND DISCUSSION

Natural convection of fluids in a vertical annulus with isothermally heated and cooled walls is studied

Table 2. Comparison of Nu_L with published results $A = 1$; $\kappa = 1$

	Nu_L		
Ra_L	(21 × 21) grid	(41 × 41) grid	Ref. [16]
10^3	1.118	1.115	1.118
10^4	2.313	2.250	2.243
10^5	4.859	4.569	4.519

$A = 10$; $\kappa = 2$ (grid: 27 × 41)

Ra_L	Present	Ref. [1]
10^4	2.355	2.333
5×10^4	3.718	3.758
10^5	4.558	4.568

numerically. The important parameters such as diameter ratio, aspect ratio and Rayleigh number have been varied and heat transfer results along with isotherms and flow fields have been obtained. New correlations are provided.

Temperature and velocity fields

The temperature profiles for $Ra_L = 2 \times 10^5$, $A = 1$ and $Z = 0.5$ are given in Fig. 2 to show the diameter ratio effect. The profiles exhibit a centro-symmetric temperature inversion about the central vertical plane for a diameter ratio of unity which represents a cavity. The temperature gradients closer to the inner wall increase and those closer to the outer cylinder are seen to decrease with the increase of diameter ratio. A dip in the temperature near $(r - r_i)/L = 0.2$ with a corresponding centro-symmetric hump closer to the outer cylinder shows the presence of two cells. The

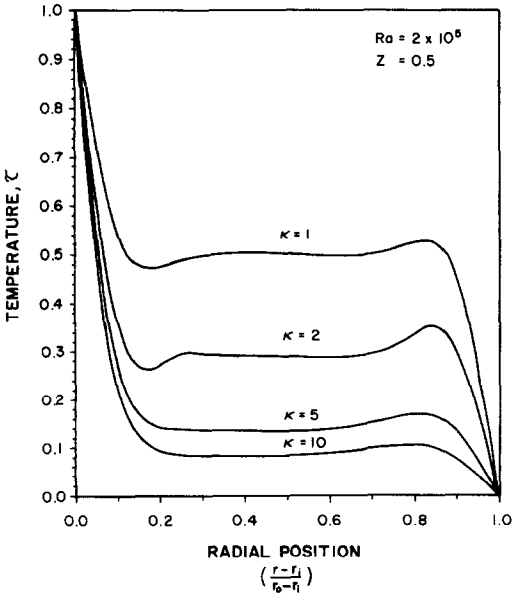

FIG. 2. Temperature profiles for $A = 1$ and $Ra_L = 2 \times 10^5$.

velocity fields given in Fig. 3 for $\kappa = 1$, $A = 1$ for three different Rayleigh numbers show that the secondary cells are not present for low Ra_L, but after they begin to appear, they become stronger at high Ra_L. For higher values of κ, the flow pattern becomes less symmetric as suggested in Fig. 4. For $\kappa = 2$, two secondary cells still exist but the isotherms deviate from symmetry. For $\kappa = 10$, there exists one primary cell, and from the isotherm plots, it is observed that with an increase in the diameter ratio, temperature decreases much faster near the hot wall and much slower near the cold wall. In other words, the hot fluid is confined to a narrow region close to the hot wall and the total percentage volume occupied by the hot fluid decreases as the diameter ratio is increased. These results will be substantiated by the local heat transfer results in the next section. The vortex center is seen to move outwards from the outer cold wall as κ is increased. The temperature profile is stratified in the core and the average core temperature decreases as the diameter ratio increases.

The isotherm and velocity field are given for a higher aspect ratio of 5 with $\kappa = 2$ and $Ra_L = 5 \times 10^4$ in Fig. 5. For the same κ, when the aspect ratio is increased, the thermals spread away from the hot cylinder and the temperature inversion is stronger near the top insulated boundary. The vortex center has also moved to this region recirculating the hot fluid. Thus, the isotherms and flow patterns given in Figs. 4 and 5 indicate that the heat transfer rate increases as the diameter ratio is increased and decreases as the aspect ratio is increased beyond unity.

Local heat transfer rate

Local Nusselt number on the hot and cold walls are presented in Fig. 6 for a square cavity. On the hot wall, the local Nu peaks at $z = 0.5$ before dropping off again. The peak increases with Ra_L indicating a reduced growth of the boundary layer for increased Rayleigh number. Near the top edge of the cold wall, the heat transfer rate is high, i.e. a high percentage of heat is rejected at a very small distance from the top. This rejection at the top edge of the outer cylinder is higher for high Rayleigh numbers.

The curvature effect on the local heat transfer rate is shown in Fig. 7 for $Ra_L = 10^5$. Once again, the local Nu increases first from $Z = 0$ and drops off near the top wall. As κ is increased, the peak Nu increases and its location shifts from the middle of the inner cylinder towards the top wall. On the outer cylinder, for all diameter ratios, a large percentage of heat is rejected at the top edge, and the local heat transfer rate decreases as κ is increased.

Heat transfer

The effects of diameter ratio and aspect ratio on the heat transfer rate are given in Figs. 8 and 9. As the diameter ratio is increased, Nusselt number increases as predicted by the isotherms in Fig. 4. It is noted that

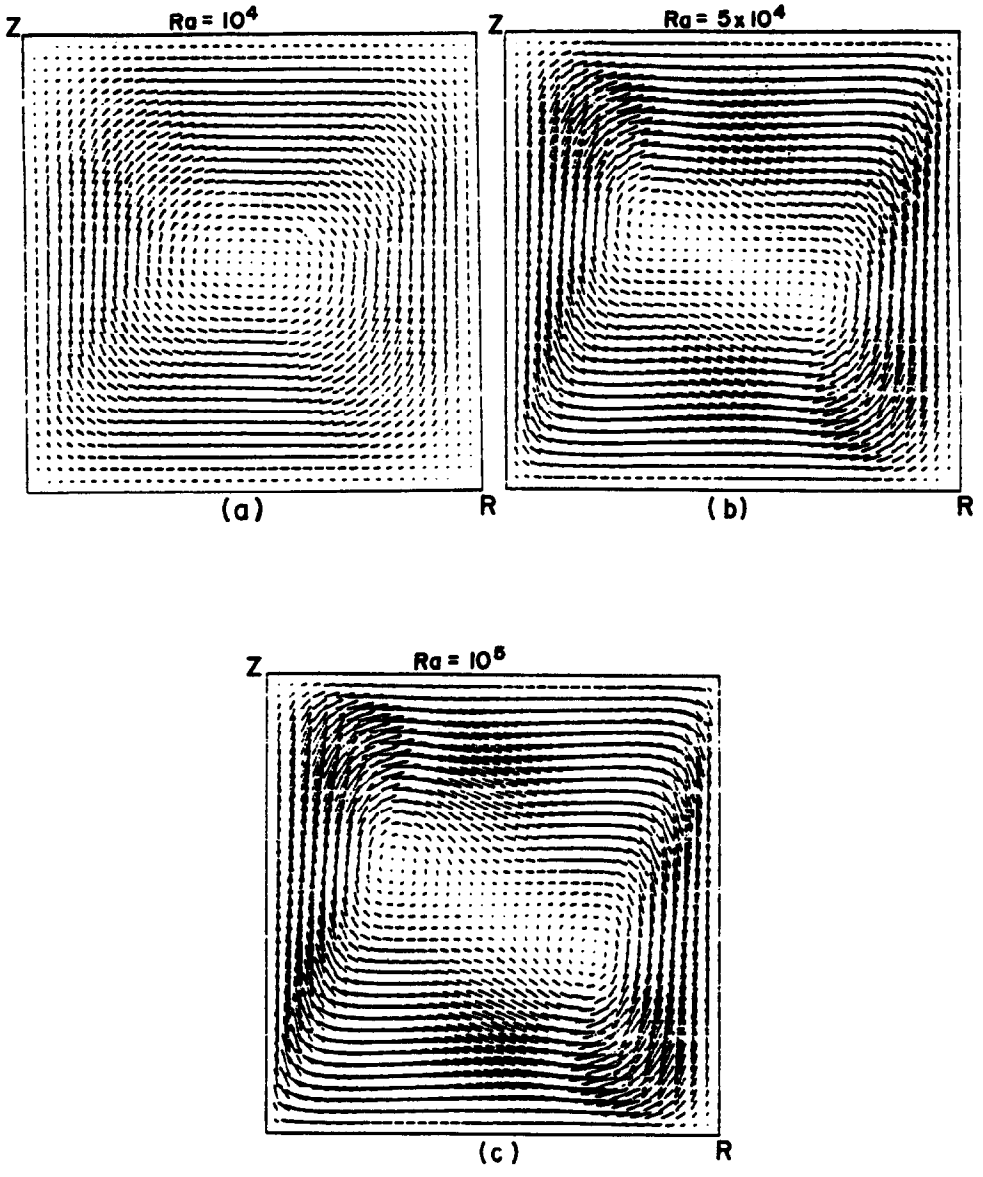

FIG. 3. Flow fields for $A = 1$, $\kappa = 1$ and (a) $Ra_L = 10^4$; (b) $Ra_L = 5 \times 10^4$; (c) $Ra_L = 10^5$.

the Nusselt number values for the conduction regime approach the asymptotic value given by

$$Nu_c = \frac{\kappa - 1}{\ln \kappa}, \quad \kappa > 1$$
$$= 1, \qquad \kappa = 1. \tag{12}$$

The conduction flow regimes are seen to be extended for higher diameter ratios. Figure 9 shows that lower heat transfer rates result as the aspect ratio is increased.

For large diameter ratios ($\kappa \geqslant 10$), the annulus behaves as a single cylinder in an infinite domain. In such cases, the inner diameter would be the appropriate length scale and would collapse the data better compared to the annulus gap width. A plot of Nu_{d_i} vs Ra_{d_i} in Fig. 10 for $A = 1$ and 10 reveals that the data for $\kappa = 10$ and 15 fall on the same line. For $A = 1$, even for a moderate diameter ratio of 5, for $Ra_{d_i} \geqslant 3 \times 10^3$, the same Nu_{d_i} values are obtained. As the aspect ratio is increased to 10, data for even low diameter ratios, $\kappa = 2$ and 5, show an asymptotic behavior at high Ra_{d_i}. These results suggest that for a high Rayleigh number and/or a high diameter ratio, the flow is predominantly a boundary layer flow and the effect of the cold cylinder is not significant. Thus, the annulus behaves as a single cylinder and the inner diameter is the appropriate length scale.

Khan and Kumar [14] showed that the same heat

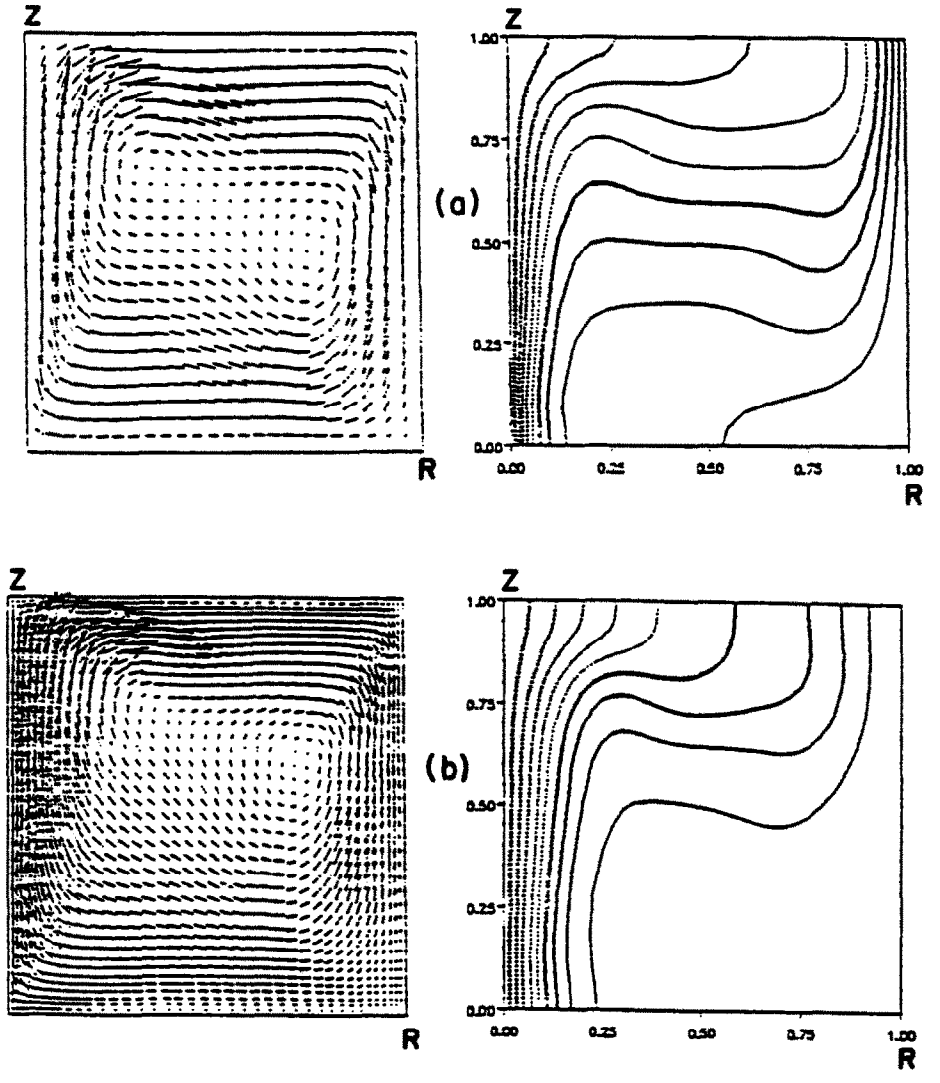

FIG. 4. Velocity field and isotherms for $A = 1$ and (a) $\kappa = 2$; (b) $\kappa = 10$.

transfer rates were predicted for isoflux and isothermal boundary conditions for high aspect ratios even if the diameter ratio was small. In light of these results, the experimental data of Keyhani *et al.* [12] for $\kappa = 4.33$ and $A = 27.6$ are plotted in Fig. 10 along with the present numerical data although their experiments were conducted with a constant heat flux boundary condition on the inner cylinder. The experimental and the numerical data for $\kappa = 5$ and $A = 10$ are in very good agreement. The implication is that the heat transfer results are independent of aspect ratio for $A \geqslant 10$ and inner cylinder boundary condition for moderate diameter ratios ($\kappa \geqslant 5$) and $Ra_{d_i} \geqslant 10^3$ in the boundary layer regime. This fact will be used later in the paper to obtain a general correlation.

The only experimental data available in the present flow configuration were provided by Prasad and Kulacki [3]. Their study was conducted for $8 \times 10^6 < Ra_L < 3 \times 10^{10}$, $\kappa = 5.338$, $A = 0.5$, 1 and 1.5, and $4 < Pr < 196$. Their temperature measurements suggest that the effective sink temperature for the boundary layer on the inner wall decreases as the radius ratio is increased. Their temperature measurements made on the top wall also suggest that the top wall is neither insulated nor perfectly conducting. For example, for $Ra = 1.6 \times 10^9$, $A = 1.0$ with water as the test fluid, the non-dimensional temperature decreased from 1.0 on the inner cylinder to 0.6 at $R = 0.25$. The temperature profile takes a linear form from $R = 0.25$ to 0.75 before it drops to zero on the outer cylinder.

Although the present numerical data were generated for a laminar, steady flow for Ra_L up to 10^6, it seems reasonable to extend the present results on the Nu_L vs Ra_L graph to $Ra_L = 2 \times 10^8$ in order to com-

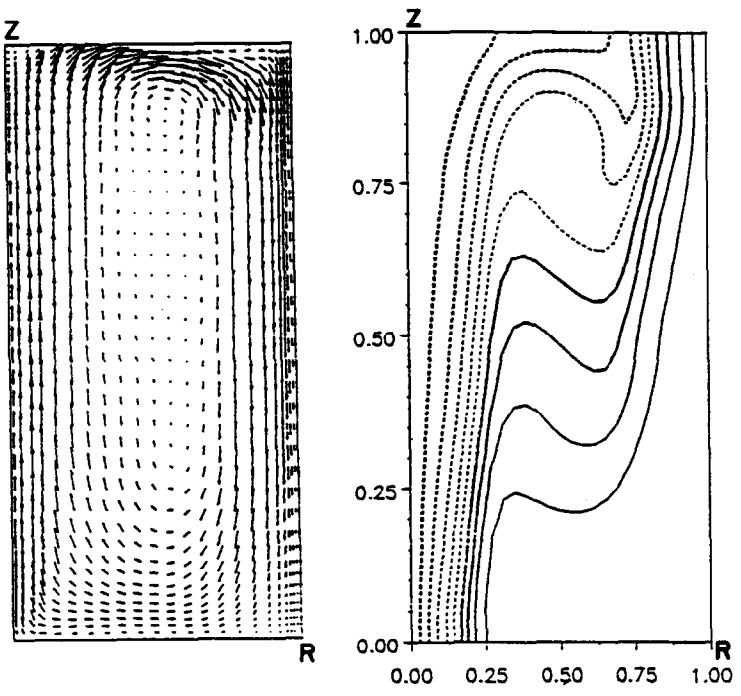

FIG. 5. Velocity field and isotherms for $A = 5$ and $\kappa = 2$.

pare them with the results given by Prasad and Kulacki [3]. In Fig. 11, the present numerical data for the insulated and perfectly conducting horizontal plates seem to envelop the experimental data with a bias towards the results for the conducting horizontal walls. It is clear from this figure that for small aspect ratios as used in the experimental study, when the heat loss through the top wall is significant, it is not reasonable to compare the experimental results with the numerical results for the insulated top and bottom walls.

In the same figure, the results of Thomas and de Vahl Davis [2] are presented using their correlation equation (1). This equation is seen to overpredict the experimental results and the present numerical results. Our results for selected parameters were compared

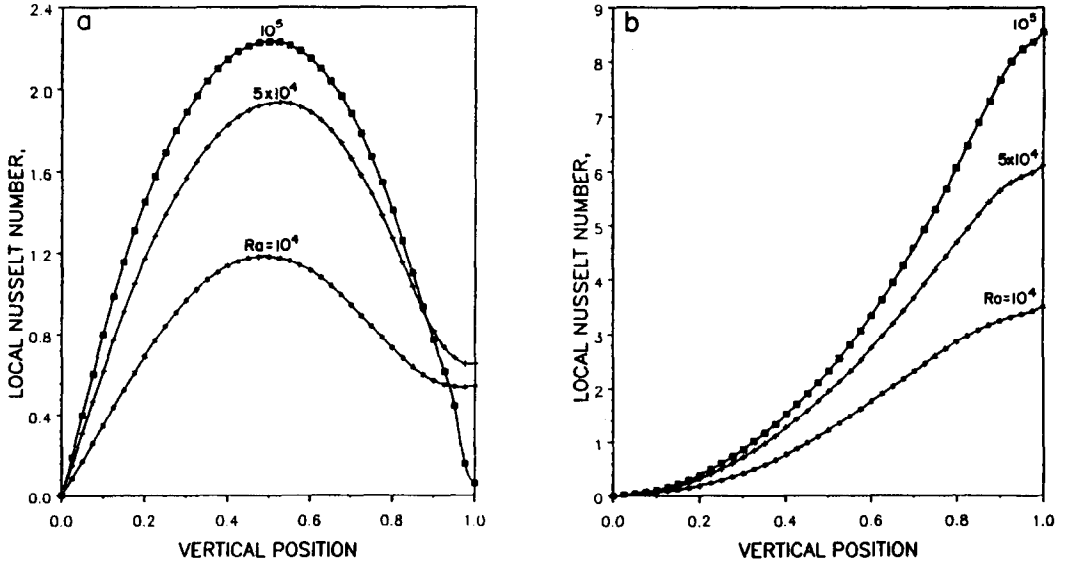

FIG. 6. Local heat transfer rate for $A = 1$ and $\kappa = 1$: (a) inner cylinder; (b) outer cylinder.

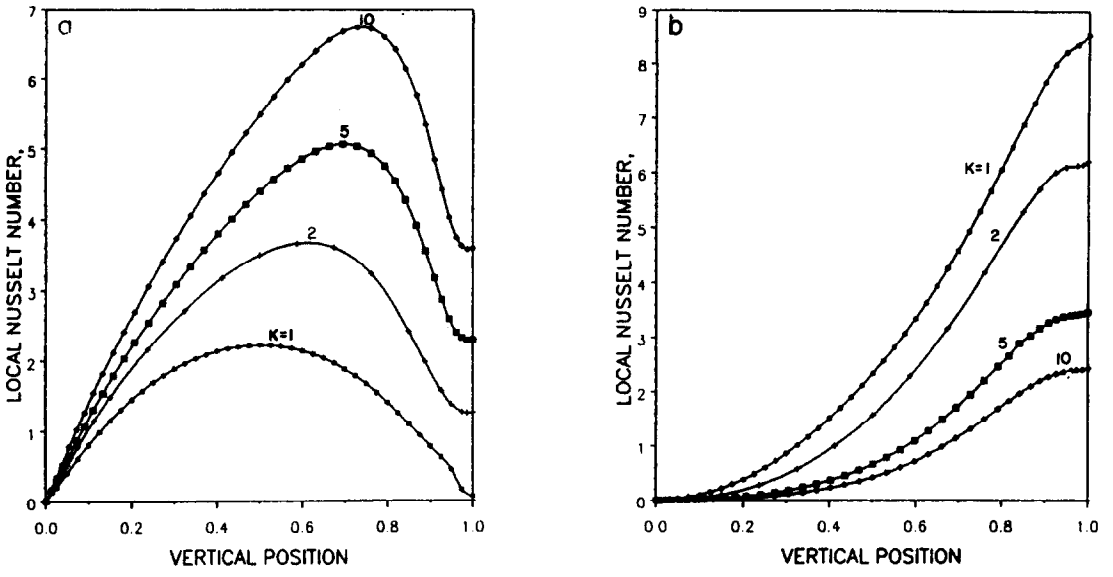

FIG. 7. Local heat transfer rate for $Ra_L = 10^5$, $A = 1$: (a) inner cylinder; (b) outer cylinder.

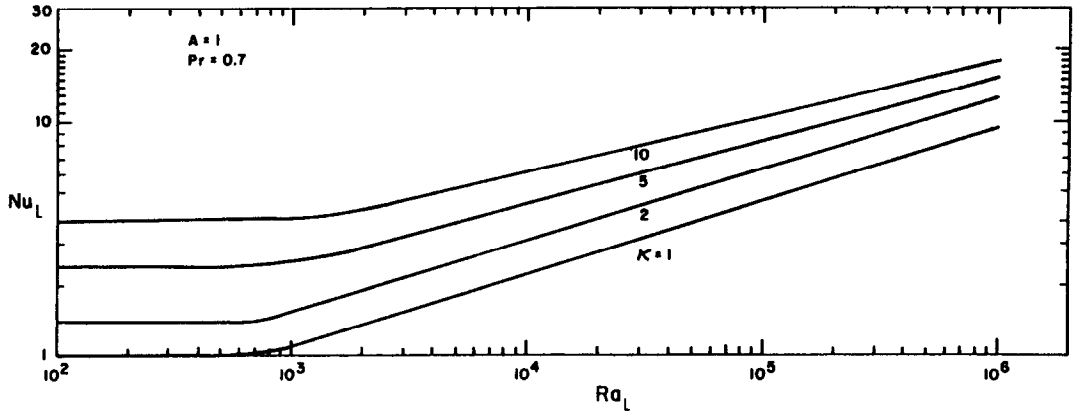

FIG. 8. Average heat transfer rate for $A = 1$ and different values of κ.

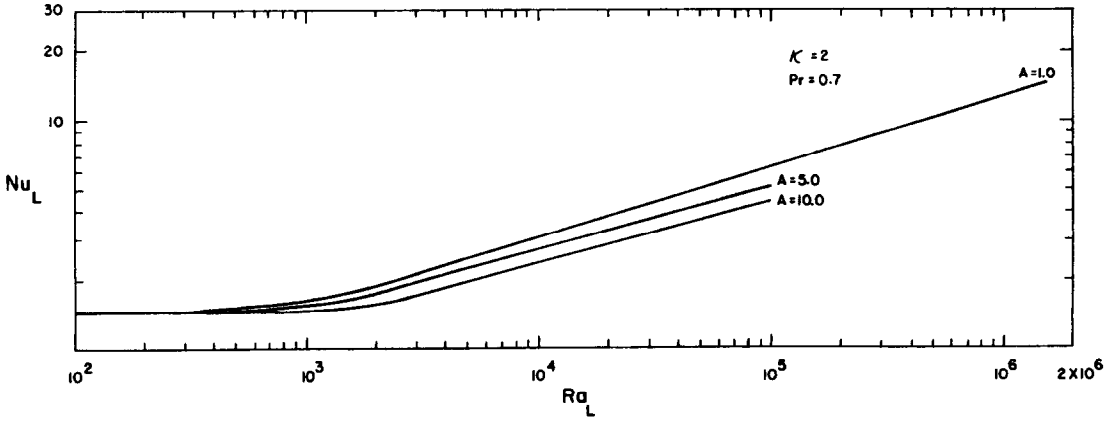

FIG. 9. Average heat transfer rate for $\kappa = 2$ and different values of A.

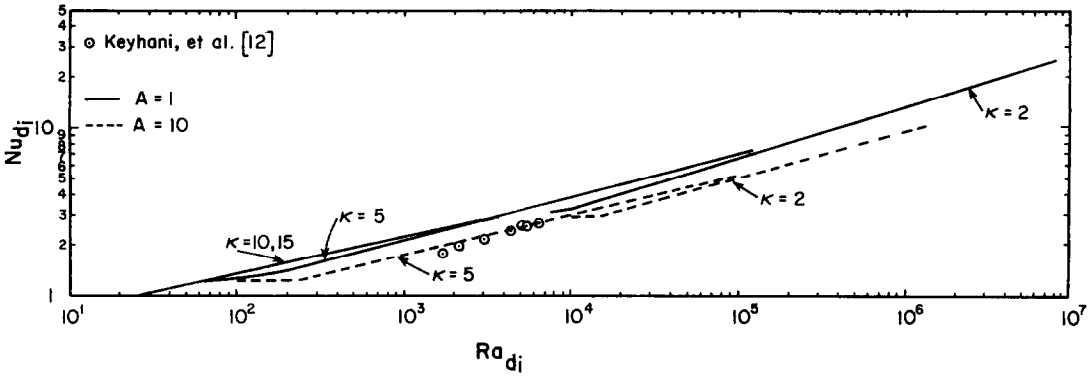

FIG. 10. Nu_{d_i} vs Ra_{d_i}.

with those of Thomas and de Vahl Davis [2] for different Ra_L, κ and A, and the agreement is excellent. (Comparison of some of these results is given in Table 2.) However, their correlation was obtained based on the majority of their results being in the range $1 \leqslant \kappa \leqslant 4$.

To understand the effect of diameter ratio and aspect ratio on Nusselt number so that an appropriate correlation may be obtained, Nu_L is plotted against κ and A in Fig. 12. The Nu_L vs κ curve has the highest slope at $\kappa = 1$ for all values of Ra_L and levels off at high diameter ratios. This suggests that the exponent of κ should be a function of κ and not merely a constant as was given by Thomas and de Vahl Davis [2]. This behavior was also seen by Prasad [18] in a vertical porous annulus. He suggested a correlation of the form

$$Nu_L = c\, Ra_L^m\, \kappa^p A^q \qquad (13)$$

where the exponent, $p \propto \kappa^{-n}$. In the present paper, it is shown that for large diameter ratios, the inner diameter is the appropriate length scale, and hence it is not necessary to obtain p which goes to zero for very high values of κ. The present data for vertical annuli may be correlated as follows:

$$Nu_L = 0.18 Ra_L^{0.278}\, \kappa^{(0.329/\kappa)+0.34} A^{-0.122} \qquad (14)$$

in the boundary layer regime for $3 \times 10^3 \leqslant Ra_L \leqslant 10^6$, $2 \leqslant \kappa \leqslant 15$, $1 \leqslant A \leqslant 10$. As κ increases, the exponent of κ decreases in equation (14) in agreement with what was observed in Fig. 12. Figure 12(b) shows that the ln (Nu) vs ln (A) may be considered linear for the purpose of correlation. Equation (14) has a standard deviation error of 4.9%. A simpler correlation may be obtained for large diameter ratios and aspect ratios using d_i as the length scale as follows:

$$Nu_{d_i} = 0.455 Ra_{d_i}^{0.202} \quad \text{for} \quad \kappa > 5,\ A \geqslant 10, \quad \text{and} \quad Ra_{d_i} > 4 \times 10^2. \qquad (15)$$

This same equation may be used for a uniform heat flux boundary condition on the inner wall as well.

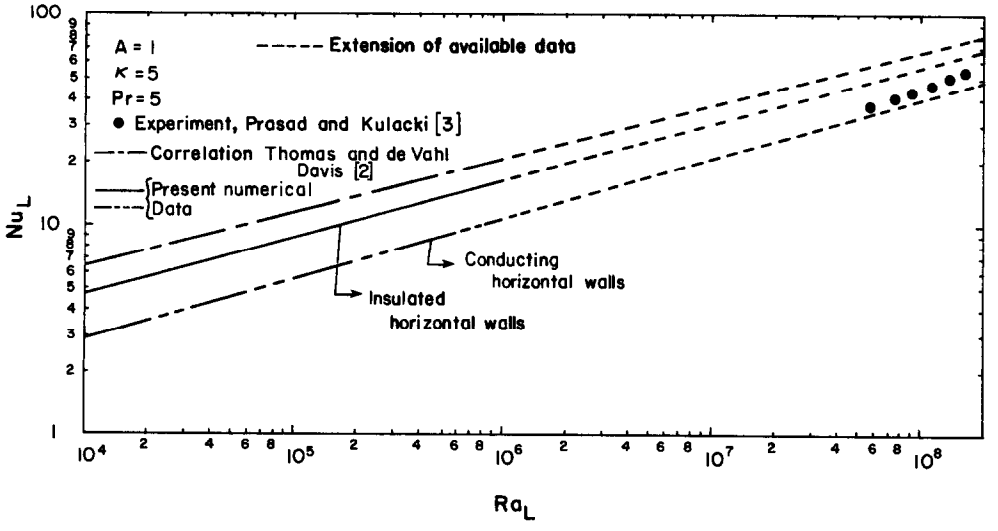

FIG. 11. Comparison of heat transfer results with data in the literature.

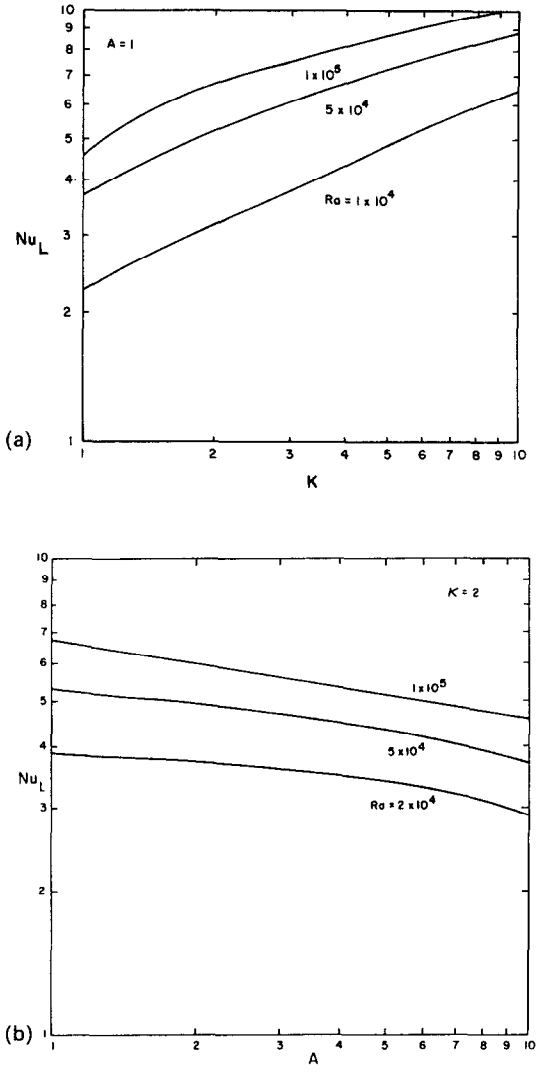

FIG. 12. (a) Nu_L vs κ. (b) Nu_L vs A.

Short cylinders

Numerical results were generated for short cylinders, i.e. $A < 1$. Since Nu_L for short cylinders is less than 1, plotting the results as Nu_L vs Ra_L as done by Prasad and Kulacki [19] for a short porous annulus or even Nu_H vs Ra_H will not bring out the physics of the problem. The lines for various aspect ratios would cross at different Rayleigh numbers making any correlation difficult to obtain. The heat transfer results for short cylinders need to be plotted as Nu_H/Nu_C (or effective thermal conductivity) vs Ra_H. The annulus height, H, is the appropriate length scale to correlate short cylinder results. These results are given for $\kappa = 5$ and $A = 0.3$, 0.5 and 1 in Fig. 13. The effect of aspect ratio is clearly delineated for all Rayleigh numbers. As the aspect ratio is increased from 0.3 to 1, the heat transfer rates decrease; the conduction flow regime also is seen to extend as A is increased from 0.5 to 1. As the diameter ratio is decreased, the curves stay similar, however, Nu_H/Nu_C increases, giving the opposite effect of tall cylinders. Thus, the need to correlate the results specially for short cylinders exists. The plots, Nu_H/Nu_C vs κ and Nu_H/Nu_C vs A were nearly linear, however the slopes for Nu_H/Nu_C vs A were considerably different for different Rayleigh numbers. Hence the exponent of Ra_H was treated as a function of A to keep the scatter in the correlation within bounds. Thus, the data for short cylinders for $Ra_H \geqslant 4 \times 10^3$ and $0.3 \leqslant A \leqslant 1$ may be presented as follows:

$$\frac{Nu_H}{Nu_C} = 0.045 Ra_H^{-0.1814+0.598} \kappa^{-0.194} A^{0.149}. \quad (16)$$

The standard deviation error in the above equation is within 10%.

Prandtl number is one of the parameters in this problem. This was kept constant at 0.7 in this study. It has been shown that the average Nusselt number is a very weak function of Prandtl number for $Pr \geqslant 0.7$ by Fujii and Verhara [20] in a vertical cylinder, McGregor and Emery [21] within vertical plates and Thomas and de Vahl Davis [2] in a vertical annulus. Hence the correlations given in equations (14)–(16) are valid for $Pr \geqslant 0.7$.

SUMMARY AND CONCLUSIONS

Numerical data have been generated in tall and short vertical annuli with isothermal cylinders and insulated top and bottom walls. Heat transfer and fluid flow results have been presented in terms of Nusselt number, isotherms and velocity field. Several combinations of parameters in the range of $0.3 \leqslant A \leqslant 10$, $1 \leqslant \kappa \leqslant 15$ and $10 < Ra_L < 10^6$ have been considered.

The existing correlation for $A \geqslant 1$ given by Thomas and de Vahl Davis [2] overpredicts the present results and the discrepancy is due to the diameter ratio effect. From the temperature plots of the experiment performed by Prasad and Kulacki [3], it is seen that the top and bottom walls were neither insulated nor perfectly conducting. The extended numerical results for both boundary conditions on the horizontal walls envelop the experimental results. However, for $\kappa \geqslant 5$ and $A \geqslant 10$, the experimental results for an isoflux inner wall of Keyhani *et al.* [12] in the Rayleigh number range of interest are in excellent agreement with the numerical data, if the data is scaled with the inner diameter instead of the annulus gap width. A simple correlation independent of κ and A is given for $\kappa \geqslant 5$ and $A \geqslant 10$.

A heat transfer correlation for tall annuli which includes an exponent of κ as another function of κ, correlates the data better.

For short cylinders, Nu_H/Nu_C vs Ra_H is seen to be the best way to plot the heat transfer results. A

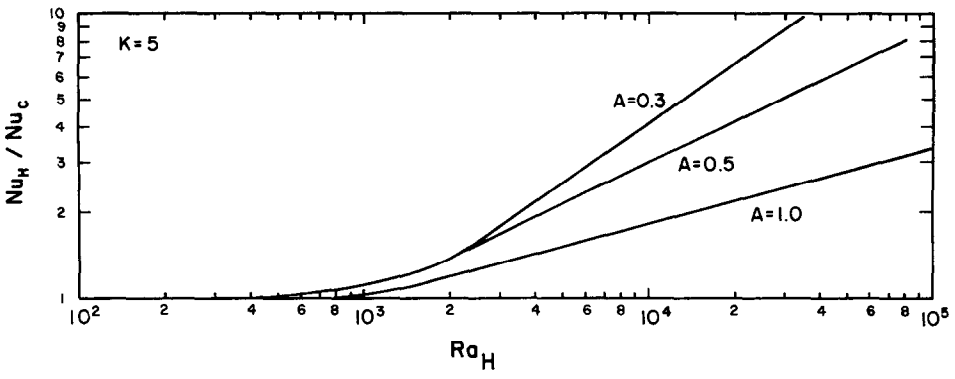

FIG. 13. Effect of short aspect ratio on heat transfer results.

correlation is given which has different characteristics compared to the one for tall annuli.

REFERENCES

1. G. de Vahl Davis and R. W. Thomas, Natural convection between concentric vertical cylinders. In *High Speed Computing in Fluid Dynamics, Physics of Fluids*, Supplement II, pp. 198–207 (1969).
2. R. W. Thomas and G. de Vahl Davis, Natural convection annular and rectangular cavities—a numerical study, *Proc. 4th Int. Heat Transfer Conf.*, Paris, Vol. 4, Paper N.C. 2.4 (1970).
3. V. Prasad and F. A. Kulacki, Free convection heat transfer in a liquid-filled annulus, *J. Heat Transfer* **107**, 596–602 (1985).
4. A. F. Emery and N. C. Chu, Heat transfer across vertical layers, *J. Heat Transfer*, Series C **87**, 110–114 (1965).
5. A. Rubel and F. Landis, A numerical study of natural convection in a vertical rectangular enclosure, *Proc. Int. Symp. on High Speed Computing in Fluid Mechanics*, Monterey, California (1968).
6. J. W. Elder, Laminar free convection in a vertical slot, *J. Fluid Mech.* **23**, 77–111 (1965).
7. Y. Lee, S. A. Korpela and R. N. Horne, Structure of multicellular natural convection in a tall vertical annulus, *Proc. 7th Int. Heat Transfer Conf.*, Munich, Vol. 2, pp. 221–226 (1982).
8. I. G. Choi and S. A. Korpela, Stability of the conduction regime of natural convection in a tall vertical annulus, *J. Fluid Mech.* **99**, 725–741 (1980).
9. H. R. Nagendra, M. A. Tirunarayanan and A. Ramachandran, Free convection heat transfer in vertical annuli, *Chem. Engng Sci.* **5**, 605–610 (1970).
10. T. H. Schwab and K. J. DeWitt, Numerical investigation of free convection between two vertical coaxial cylinders, *A.I.Ch.E. Jl* **16**, 1005–1010 (1970).
11. N. Sheriff, Experimental investigation of natural convection in single and multiple vertical annuli with high pressure carbon dioxide, *Proc. 3rd Int. Heat Transfer Conf.*, Chicago, Vol. 2, pp. 132–138 (1966).
12. M. Keyhani, F. A. Kulacki and R. N. Christensen, Free convection in a vertical annulus with constant heat flux on the inner wall, *ASME J. Heat Transfer* **105**, 454–459 (1983).
13. R. Bhushan, M. Keyhani, R. N. Christensen and R. A. Kulacki, Correlation equations for free convection in a vertical annulus with constant heat flux on the inner wall, *ASME J. Heat Transfer* **105**, 910–912 (1983).
14. J. A. Khan and R. Kumar, Natural convection in vertical annuli: a numerical study for constant heat flux on the inner wall, *ASME J. Heat Transfer* **111**, 909–915 (1989).
15. A. A. Samarskii and V. B. Andreyev, On a high accuracy difference scheme for an elliptic equation with several space variables, *USSR Comp. Math. Math. Phys.* **3**, 1373–1382 (1963).
16. G. de Vahl Davis, Finite difference methods for natural and mixed convection in enclosures, *Proc. 8th Int. Heat Transfer Conf.*, San Francisco, Keynote Paper, Vol. 1, pp. 101–109 (1986).
17. G. de Vahl Davis, Natural convection of air in a square cavity: a bench mark numerical solution, *Int. J. Numer. Meth. Fluids* **3**, 249–264 (1983).
18. V. Prasad, Numerical study of natural convection in a vertical porous annulus with constant heat flux on the inner wall, *Int. J. Heat Mass Transfer* **6**, 841–854 (1986).
19. V. Prasad and F. A. Kulacki, Natural convection in porous media bounded by short concentric vertical cylinders, *J. Heat Transfer* **107**, 147–154 (1985).
20. T. Fujii and H. Verhara, Laminar natural convective heat transfer from the outer surface of a vertical cylinder, *Int. J. Heat Mass Transfer* **13**, 607–615 (1970).
21. R. K. McGregor and A. F. Emery, Free convection through vertical plane layers—moderate and high Prandtl number fluids, *J. Heat Transfer* 391–403 (1969).

CONVECTION THERMIQUE LAMINAIRE ENTRE DES CYLINDRES VERTICAUX, COAXIAUX ET ISOTHERMES

Résumé—On étudie numériquement la convection naturelle d'un fluide dans un espace cylindrique vertical avec la paroi intérieure maintenue à une température supérieure à celle de la paroi extérieure. Le sommet et la base sont isolés dans la majorité des cas. On considère aussi des parois parfaitement conductrices pour comparer les résultats du transfert thermique. Sont donnés les résultats numériques sur les flux thermiques et les champs de vitesse pour $10 \leqslant Ra_L \leqslant 10^6$, $1 \leqslant \kappa \leqslant 15$ et $0{,}3 \leqslant A \leqslant 10$. On note et discute des écarts entre les résultats numériques et les données expérimentales. On donne de nouvelles formules pour le flux thermique.

LAMINARE THERMISCHE KONVEKTION ZWISCHEN SENKRECHTEN KOAXIALEN ISOTHERMEN ZYLINDERN

Zusammenfassung—Die natürliche Konvektion in einem senkrechten zylindrischen Ringspalt wird für den Fall numerisch untersucht, daß die Wand des Innenzylinders eine höhere Temperatur aufweist als die des Außenzylinders. In den meisten Fällen sind die oberen und unteren Stirnflächen wärmegedämmt. Zum Vergleich werden auch ideal leitende horizontale Wände betrachtet. Strömung und Wärmeübergang werden für folgende Parameterbereiche berechnet: $10 \leqslant Ra_L \leqslant 10^6$; $1 \leqslant \kappa \leqslant 15$; $0{,}3 \leqslant A \leqslant 10$. Unterschiede zwischen vorhandenen numerischen Ergebnissen und den Versuchsdaten werden registriert und diskutiert. Schließlich werden neue Korrelationsgleichungen für den Wärmeübergang angegeben.

ЛАМИНАРНАЯ ТЕПЛОВАЯ КОНВЕКЦИЯ МЕЖДУ ВЕРТИКАЛЬНЫМИ СООСНЫМИ ИЗОТЕРМИЧЕСКИМИ ЦИЛИНДРАМИ

Аннотация—Численно исследуется естественноконвективный теплоперенос жидкости в вертикальных цилиндрических кольцевых каналах, на внутренней стенке которых поддерживается более высокая температура, чем на внешней. В большинстве случаев верхняя и нижняя пластины теплоизолированы. Для сравнения результатов теплопереноса исследуются также идеально проводящие горизонтальные стенки. Приводятся численные результаты для тепловых потоков и полей течения в диапазоне $10 \leqslant Ra_L \leqslant 10^6$, $1 \leqslant \kappa \leqslant 15$ и $0{,}3 \leqslant A \leqslant 10$. Отмечаются и обсуждаются расхождения в имеющихся численных и экспериментальных данных. Предложены новые соотношения для тепловых потоков.